Available online at www.sciencedirect.com
SCIENCE DIRECT®
International Journal of Solids and Structures 42 (2005) 2625–2644
INTERNATIONAL JOURNAL OF SOLIDS and STRUCTURES
www.elsevier.com/locate/ijsolstr

On description of hysteretic behaviour of materials

Grigori Muravskii *

Faculty of Civil Engineering, Israel Institute of Technology, Technion, 32000 Haifa, Israel

Received 25 May 2004; received in revised form 6 October 2004
Available online 23 November 2004

Abstract

In the paper, a modification of well known extended Masing's rules is suggested in order to provide more flexible description of stress–strain relationships of different materials. Particularly, the modification allows us to regulate the dependence of the damping ratio on the strain amplitude in the process of cycle deforming of a material. As the four extended Masing's rules have a good mechanical basis in models of Iwan's type, it is appropriate to retain whenever possible the main context of these rules. The suggestion consists only in modification of the second rule, in which instead of the scaled backbone curve another function is considered. The two cases of hysteretic systems are studied: the system with limited stress when strain increases without bound, and the system with constant stiffness (linear backbone curve) into which hysteretic properties are introduced. For a number of dynamic examples, a comparison of different hysteretic models is carried out.

Keywords: Hysteresis; Masing's rules; Hysteresis function; Damping ratio; Hysteretic loop

1. Introduction

The well known extended Masing's rules, defining relationships between stress τ and strain γ, are based on the behaviour of a mechanical system comprising large (infinite) number of Prandtl's elements (joined in parallel) or the elements, each of which consists of a spring in parallel with a Coulomb's slider, joined in series. Actually, the first variant of the system has been used by Masing (1926) for derivation of his rules (the two rules of the four extended rules). The above models are called in publications as Iwan's models (Iwan, 1966; Iwan, 1967) although they were known much earlier. It seems appropriate to give here the formulation of the four extended Masing's rules (Kramer, 1996)

* Tel.: +972 4829 2271; fax: + 972 4823 7149.
E-mail address: gmuravsk@tx.technion.ac.il

0020-7683/$ - see front matter © 2004 Elsevier Ltd. All rights reserved.
doi:10.1016/j.ijsolstr.2004.10.009

1. For initial loading, the stress–strain curve follows the backbone curve $\tau = F_{\mathrm{bb}}(\gamma)$.
2. If a stress reversal occurs at a point defined by $(\gamma_{\mathrm{rev}}, \tau_{\mathrm{rev}})$, the stress–strain curve follows a path given by

$$\frac{\tau - \tau_{\mathrm{rev}}}{2} = F_{\mathrm{bb}}\left(\frac{\gamma - \gamma_{\mathrm{rev}}}{2}\right) \tag{1}$$

3. If the unloading or reloading curve exceeds the maximum past strain and intersects the backbone curve, it follows the backbone curve until the next stress reversal.
4. If an unloading or reloading curve crosses an unloading or reloading curve from the previous cycle, the stress–strain curve follows that of the previous cycle.

Regarding the third rule, note that it relates also to the case when maximum past strain, but with opposite sign, is exceeded. The attempts to modify the Masing's rules have been made among others by Pyke (1979), Archuleta et al. (1999) and Osinov (2003). Pyke (1979) retains only the first rule and uses for subsequent loadings and unloadings, hyperbolic curves with an asymptotes defined by strength of the material. Advantages of such a treatment consist in simplicity of tracking the stress–strain relationship, and in limitation of stresses by the strength of the considered material. Let us consider how a departure from Masing's rules can lead to significant changes in the behaviour of the model. Assume, e.g. that the backbone curve is a hyperbola with an initial modulus $G_{\max}$ and limit stress τ_u

$$y = \frac{x}{1+x} \tag{2}$$

where x and y are the normalized strain and stress, respectively, which are defined by a strain γ and stress τ as follows:

$$x = \frac{\gamma}{\gamma_r}, \quad y = \frac{\tau}{\tau_u}, \quad \gamma_r = \frac{\tau_u}{G_{\max}} \tag{3}$$

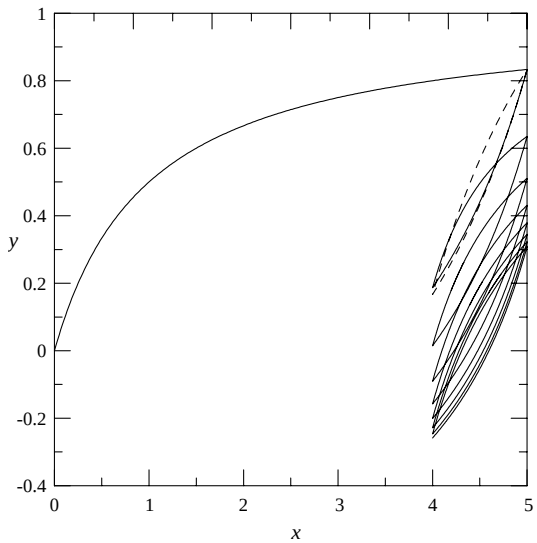

Fig. 1. Example to Pyke's model: non-symmetrical cycles for deformation result in symmetry for stresses. Dashed line represents model obeying Masing's rules.

Such normalization is desired for any backbone curve with limited strength. Consider for backbone curve (2) strain controlled deforming beginning from $x = 0$ and having repeatedly reversal points at $x = 5$ and $x = 4$. According to Pyke's model, we obtain the stress–strain relationship shown in Fig. 1. With increase in number of cycles stresses become symmetrical; such behaviour differs from that of Masing's model represented by the dashed line in Fig. 1. Note that Pyke's model appears to be suitable for description of the behaviour of granular materials in processes of deformation like described above. The second example relates to the following series of reversal points: $x = 2j,\ 2j - 0.1$ $(j = 1, 2, \ldots)$. The stress–strain curve is represented in Fig. 2 where the dashed line corresponds to the Masing's model. The disposition of loading and unloading parts of the stress–strain curve for Pyke's model indicates on the violation of Drucker's stability postulate (see Shames and Cozzarelli, 1992; Goodier and Hodge, 1958) which states in essence that energy put into plastic deformation cannot be recovered. Consider an initial equilibrium of a body corresponding to point A (Fig. 3). Let some external agency apply an additional force to the body and then remove it. The corresponding process could be represented by the unloading path AB and reloading path BC. According to Drucker's postulate, the work done by the external agency (i.e. by additional stresses) is non-negative. This leads to the relationship $E_1 \geqslant E_2$ where E_1 and E_2 areas indicated in Fig. 3. Parts of stress–strain history represented by solid line in Fig. 2 do not satisfy this requirement. The behaviour similar to that of Pyke's model is observed in other models, e.g. suggested by Osinov (2003), Archuleta et al. (1999), Bouc–Wen model (Bouc, 1967; Wen, 1976).

One of the important characteristics of a model is the damping ratio corresponding to symmetric cyclic deforming of a material. Classical Masing's model as well as such models as Pyke's model do not allow regulating this parameter which in practice can be smaller than that predicted by the models. Model of Archuleta et al. allows weak regulating the damping making it however too large. The models suggested by Muravskii and Frydman (1998), Muravskii (2001) and Osinov (2003) are intended for eliminating above shortcomings.

In the paper, some hysteretic models are constructed which differ from the model obeying four extended Masing's rules only in the second rule: instead of the scaled backbone curve (1), a function $\Phi(u)$ satisfying some requirements is applied. Eq. (1) is taken in the form

$$\tau = \tau_{\mathrm{rev}} + \Phi(\gamma - \gamma_{\mathrm{rev}}) \tag{4}$$

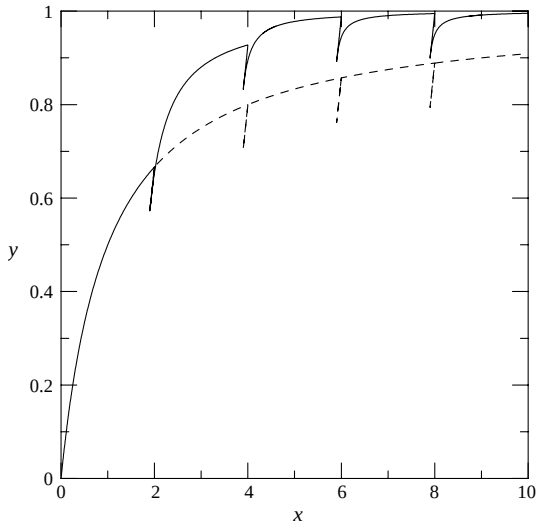

Fig. 2. Loadings and unloadings with increasing reversal strains for Pyke's model and model corresponding to Masing's rules (dashed line).

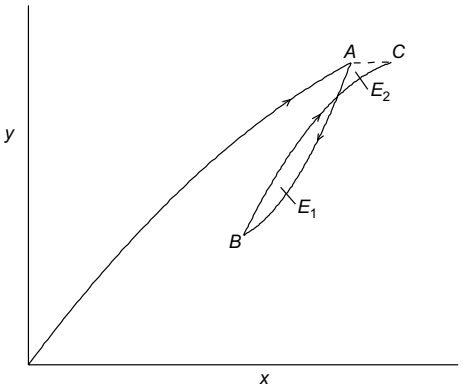

Fig. 3. On Drucker's postulate.

Note that the function $\Phi(u)$ corresponding to Eq. (1) has the form

$$\Phi(u) = 2F_{\mathrm{bb}}(u/2) \tag{5}$$

Function $\Phi(u)$ will be called hysteresis function.

2. Constructing hysteresis function for material with limited strength

The function Φ should satisfy (similarly to the backbone curve) the condition of antisymmetry, i.e. $\Phi(-u) = -\Phi(u)$, and contain as a parameter the absolute values of strain, γ_{bb}, at which the point (γ, τ) leaves the backbone curve because of unloading or reloading. This parameter remains without changes until the point (γ, τ) starts to move again along the backbone curve (according to the third rule) and afterwards abandons it at a new value γ_{bb}. For symmetric cycle deforming, the amplitude of deformations equals the parameter γ_{bb}. An important property of the relationship (4) with the condition of antisymmetry mentioned above is that after an unloading with a following reloading a point comes back into the reversal point where the unloading began (similarly to the classic Masing's model). In addition, the following requirements are imposed on the function Φ and its derivatives

$$\begin{aligned}
&\text{(i)}\ \Phi(0) = 0\\
&\text{(ii)}\ \Phi'(0) = F'_{\mathrm{bb}}(0)\\
&\text{(iii)}\ \Phi(2\gamma_{\mathrm{bb}}) = 2\tau_{\mathrm{bb}}\\
&\text{(iv)}\ \Phi'(2\gamma_{\mathrm{bb}}) = F'_{\mathrm{bb}}(\gamma_{\mathrm{bb}})\\
&\text{(v)}\ \Phi'(u) > 0 \quad \text{and} \quad \Phi''(u) < 0 \quad \text{for } 0 \leqslant u \leqslant 2\gamma_{\mathrm{bb}}
\end{aligned} \tag{6}$$

where $\tau_{\mathrm{bb}} = F_{\mathrm{bb}}(\gamma_{\mathrm{bb}})$. All these relationships stem from the properties of the scaled backbone curve entering the Eqs. (1) and (5). When using normalized values according to (3) γ and τ are changed to x and y, respectively, in above relationships; in this case initial derivative in (ii) equals one. Additional parameters which can enter function Φ allow us to regulate its behaviour in intermediate parts of the interval $(0, 2\gamma_{\mathrm{bb}})$ and thus to influence the form of hysteresis loops and damping properties of the model.

Using normalized strain and stress x, y, consider as an illustration two simple functions for constructing function Φ, logarithmic function suggested by Puzrin and Burland (1996)

$$\Phi(u) = u\{1 - \alpha[\ln(1 + |u|)]^R\} \tag{7}$$

and function used by Davidenkov (1938)

$$\Phi(u) = u(1 - \alpha|u|^R) \tag{8}$$

Requirements (i), (ii), (v) in (6) are satisfied. For the logarithmic function (7) we obtain from (iii) and (iv)

$$R = \frac{[y_{bb} - x_{bb}F'_{bb}(x_{bb})](1 + 2x_{bb})\ln(1 + 2x_{bb})}{2x_{bb}(x_{bb} - y_{bb})} \tag{9}$$

$$\alpha = \frac{x_{bb} - y_{bb}}{x_{bb}[\ln(1 + 2x_{bb})]^R} \tag{10}$$

For function (8), parameters R and α are as follows:

$$R = \frac{[y_{bb} - x_{bb}F'_{bb}(x_{bb})]}{x_{bb} - y_{bb}} \tag{11}$$

$$\alpha = \frac{x_{bb} - y_{bb}}{x_{bb}(2x_{bb})^R} \tag{12}$$

Eqs. (9)–(12) show explicitly how parameter x_{bb}, defined as absolute value of the normalized strain at which the backbone curve is abandoned by the point (x, y) because of unloading or reloading, enters function Φ. Practically, the suggested method (besides flexibility in choosing function Φ) differs from that based on original four extended Masing's rules only in necessity to fix parameter γ_{bb} (or x_{bb}) and use it at corresponding stages of the deformation history. In Fig. 4(a) and (b) hysteresis loops corresponding to function (5), (7) and (8) are shown in the case of hyperbolic backbone curve (2) for values of strain amplitude $x_{bb} = 5, 10$; dashed lines represent the backbone curve. In Fig. 5, the damping ratio D defined as the loop area divided by $2\pi x_{bb}y_{bb}$ is represented as a function of the strain amplitude x_{bb} for the three considered hysteresis functions. We see that the energy dissipation corresponding to large strain amplitudes is significantly smaller for functions (7) and (8) than for Masing's function (5), whereas in the case of small amplitudes, results for all the functions are closely related. These hysteresis functions do not allow regulating the damping ratio of a material because of small number of parameters. Note that functions (7) and (8) are more suitable for soils than the Masing's function (5) which leads to the limit value (for infinite amplitudes x_{bb}) of damping ratio D_{max} equal to $2/\pi$. Experiments (e.g. Hardin and Drnevich, 1972a; Hardin and Drnevich, 1972b) give the maximum values of damping ratio lying in a vicinity of 0.3.

For more flexible description of the hysteretic behaviour of a model, one can apply functions having more parameters than the functions described above. Consider the function suggested by Muravskii (1996)

$$\Phi(u) = d_1u + \frac{(d_0 - d_1)t}{1 + g|t|^R}, \quad t = u(1 - \beta|u|^q) \quad (R, q, \beta > 0, g \geqslant 0) \tag{13}$$

where d_1 is set equal to the derivative at the end point $u = u_E = 2\gamma_{bb}$ of the considered interval $(0, u_E)$ according to (iv), d_0 is the derivative at $u = 0$ ($d_0 = 1$ in the case of the above normalization). The requirement (iv) for the derivative $\Phi'(u)$ at the point u_E leads to

$$\beta = \frac{1}{(1 + q)u_E^q} \tag{14}$$

which follows from the condition that the derivative t by u must be zero at the point. The Eq. (iii) in (6) allows defining parameter g

$$g = \frac{(t_E/u_r) - 1}{t_E^R} \tag{15}$$

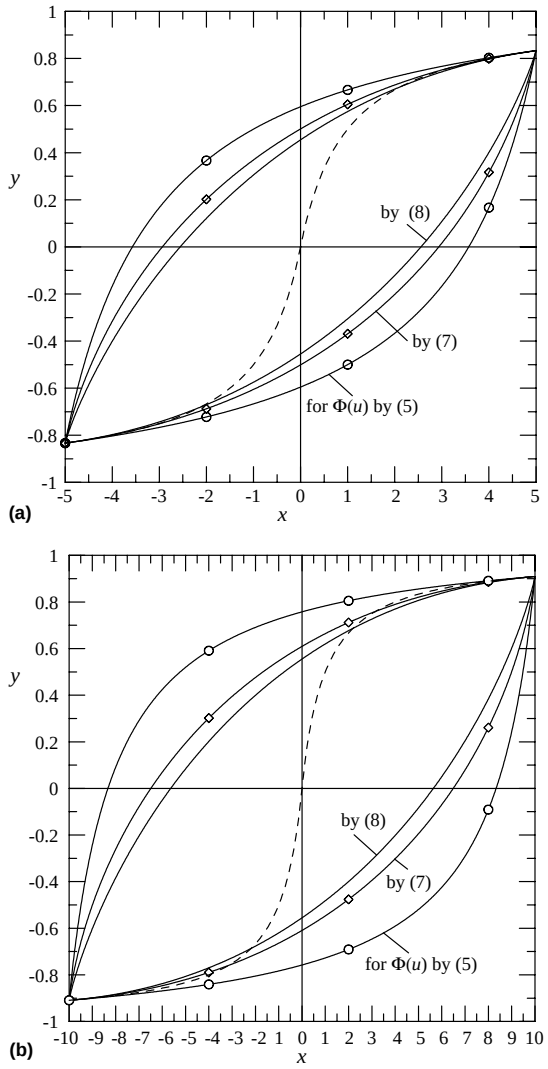

Fig. 4. Hysteresis loops corresponding to hysteresis function (5), (7) and (8) in the case of hyperbolic backbone curve (2) for 2 values of strain amplitude $x_{bb} = 5$ (a) and 10 (b).

where

$$t_E = u_E(1 - \beta u_E^q) = \frac{q u_E}{q+1} = \frac{2q\gamma_{bb}}{q+1} \tag{16}$$

$$u_r = \frac{\Phi(u_E) - d_1 u_E}{d_0 - d_1} = 2\frac{\tau_{bb} - d_1\gamma_{bb}}{d_0 - d_1} \tag{17}$$

The condition $g \geqslant 0$ leads to

$$q \geqslant q_0 = \frac{1}{(u_E/u_r) - 1} \tag{18}$$

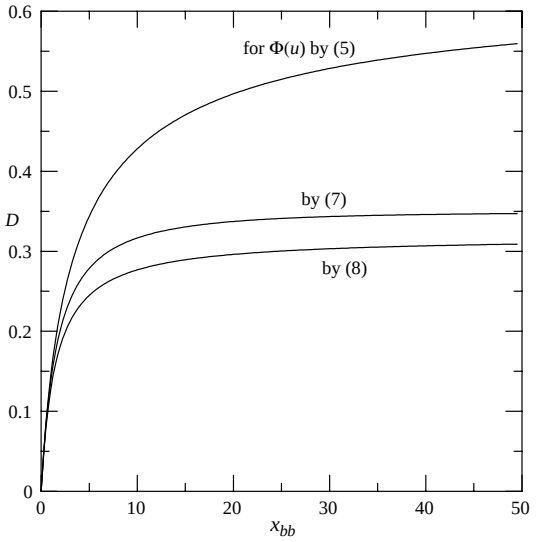

Fig. 5. Damping ratio D as a function of the strain amplitude x_{bb} for the three considered hysteretic functions (5), (7) and (8).

If $q = q_0$ then $g = 0$, and the considered function has the form of Davidenkov's function (8). A limitation for parameter R following from requirement (v) in (6) is (Muravskii, 1996)

$$R \leqslant R_0 = \frac{1}{1 - u_r(q+1)/(u_E q)} \tag{19}$$

We see that after satisfying relationships (6) due to defining parameters β and g according to (14) and (15), the two free parameters, q and R, remain. They can be used for regulating function properties in intermediate points of the interval $(0, u_E)$. The value of R_0 is greater than one and tends to one with increase in u_E. First consider the relationship between R and the damping ratio of the model for very large values of the normalized strain amplitude x_{bb}, when independently of the form of a backbone curve one can take normalized stress $y_{\mathrm{bb}} = 1$, $F'_{\mathrm{bb}}(x_{\mathrm{bb}}) = 0$. Choosing normalized strain amplitude $x_{\mathrm{bb}} = 10{,}000$, calculations of damping ratio have been made for values of $R = R^*$ (the notation indicates that the parameter is related to the taken large amplitude) from interval $0 < R^* \leqslant 1$ and the following values of q

$$q = \frac{q_0 + 2}{R} \tag{20}$$

Thus limitations (18) and (19) have been taken into account. In Fig. 6 the values R^* are presented as a function of the values $D_{\max}$ of damping ratio for $x_{\mathrm{bb}} = 10{,}000$. $D_{\max}$ can be considered practically as maximum values i.e. relating to infinite strain amplitudes. For $R^* = 1$ the value $D_{\max} = 0.6355$ which is close to the mentioned above limit value $2/\pi$ or 0.6366. Underline that the results represented in Fig. 6 are independent of the kind of a backbone curve with limited strength. The function of Fig. 6 allows the following very precise polynomial approximation

$$R^* = 1.5532 D_{\max} + 1.5819 D_{\max}^2 - 3.6843 D_{\max}^3 + 1.9601 D_{\max}^4 \tag{21}$$

The curve representing this equation practically coincides with the curve in Fig. 6 obtained with above calculations.

Defining damping ratio for different values of strain amplitudes x_{bb} we can change parameters R with changes in x_{bb} or use constant value $R = R^*$. As an example, let us retain $R = R^*$ for all values of strain

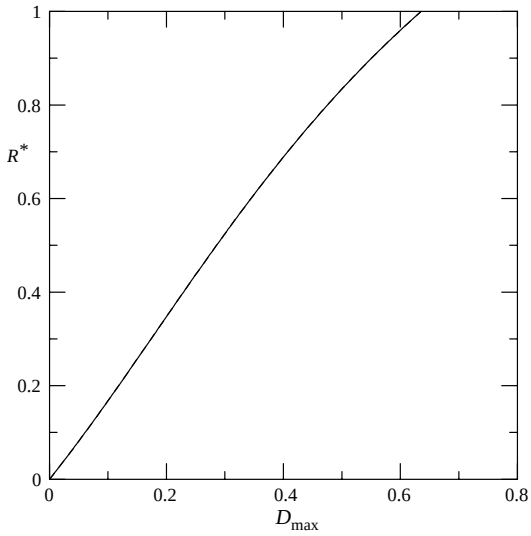

Fig. 6. Values of parameter R^* for normalized strain amplitude $x_{bb} = 10{,}000$, versus damping ratio D_{max}; dashed line corresponds to Eq. (21).

amplitudes keeping q by (20). As a result we obtain the damping ratio dependence on the strain amplitude shown in Fig. 7 for values of $D_{max} = 0.1$, 0.2, 0.3, 0.4, 0.5, 0.6355 and the corresponding values of R^* defined according to (21) $R^* = 0.167651$, 0.347578, 0.524732, 0.688767, 0.834044, 1.00004 (hyperbolic backbone curve is used). The dashed line in Fig. 7 represents results relating to the original four extended Masing's rules with the hyperbolic backbone curve. Note that in the case with R depending on the normalized strain amplitude according to the equation

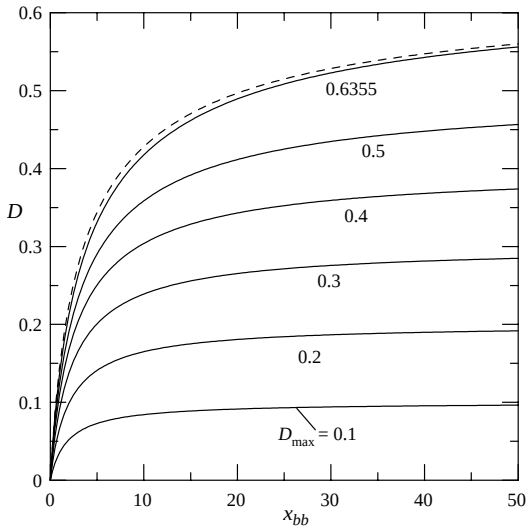

Fig. 7. Damping ratio dependence on strain amplitude in the case $R = R^*$ for different maximum values of damping ratio (hyperbolic backbone curve); dashed line corresponds to the original four extended Masing's rules.

$$R = R^* \frac{1.3 + x_{bb}}{1 + x_{bb}} \tag{22}$$

the dashed line and the line for $R^* = 1$ ($D_{max} = 0.6355$) in Fig. 7 merge with each other. Also the corresponding hysteretic loops will be in this case practically identical for any value of strain amplitudes.

For a given value of D_{max} parameter R^* can be found using Eq. (21), and afterwards one can obtain the required curve which relates damping ratio to strain amplitude. Apparently, Eq. (20) for q and value R in the form

$$R = R^* \frac{A + x_{bb}}{B + x_{bb}} \tag{23}$$

can be recommended. The positive constants A and B allow us to regulate behaviour of the damping ratio at small and intermediate values of the normalized strain amplitude x_{bb}.

3. Comparison some hysteretic models allowing damping regulation

Besides the model constructed in this paper consider additional two models which are capable to describe not only stiffness but also damping properties of a material: quasi hysteretic model (Muravskii, 1994; Muravskii and Frydman, 1998) and elasto-hysteretic model (Muravskii, 2001). In the elasto-hysteretic model the stress is taken in the form

$$\tau = \lambda \tau_h + (1 - \lambda) F_{bb}(\gamma) \quad (0 \leqslant \lambda \leqslant 1) \tag{24}$$

where τ_h is the stress corresponding to Masing's model with $F_{bb}(\gamma)$ as backbone curve. The second term in (24) represents elastic part of the model. It is possible to regulate the maximum value D_{max} of damping ratio by variation of parameter λ however the behaviour of the damping ratio for intermediate values of strain amplitudes remain similar to that for the pure Masing's model (with coefficient λ).

The constitutive equation for quasi hysteretic model has the form

$$\tau = C_{deg} G(\gamma_m) \left[\gamma + \eta(\gamma_m) \frac{\gamma_m}{\dot{\gamma}_m} \dot{\gamma} \right] \tag{25}$$

where C_{deg} is coefficient of degradation (see Muravskii, 1994; Muravskii and Frydman, 1998) $G(\gamma_m)$ and $\eta(\gamma_m)$ two function depending on mean value (relative to time) of strain γ_m; $\dot{\gamma}$ and $\dot{\gamma}_m$ are strain rate and mean value of strain rate, respectively. In the further examples, $C_{deg} = 1$. The weighted mean value is determined as follows:

$$z_m = \left[\frac{(n+1)}{t^{n+1}} \int_0^t s^n z^2(s) \mathrm{d}s \right]^{1/2}, \quad (z = \gamma, \dot{\gamma}) \tag{26}$$

As the parameter n is made greater than 0, correspondingly more relative weight is given to data close to time t. Eq. (25) leads to frequency independent loss of energy for steady-state harmonic processes; corresponding hysteretic loops have elliptic forms. The name 'quasi hysteretic' appears to be suitable since the rate of strain is included in constitutive Eq. (25), whereas the term 'hysteresis' is understood here as rate independent behaviour (we apply the definition used in book by Visintin (1994): hysteresis = rate independent memory effect). Note that frequency independent damping is often referred to as hysteretic or ideal hysteretic damping in contrast to viscous damping (see Muravskii, 2004). In papers by Muravskii (1994), Muravskii and Frydman (1998) is shown how to construct the function $G(\gamma_m)$ and $\eta(\gamma_m)$ in order to obtain the needed behaviour for secant shear modulus and damping ratio in a cyclic process of deformation. The quasi hysteretic model allows us to satisfy more precisely experimental data on damping than

the elasto-hysteretic model which has only one parameter, λ, influencing the damping behaviour of the model in cyclic processes.

Let us compare shapes of hysteretic loops for the three considered models. To make all the models equivalent regarding to the damping behaviour, the dependence of damping ratio on strain amplitudes for the new model and the quasi hysteretic model is adjusted to the elasto-hysteretic model, i.e. (for the hyperbolic backbone curve)

$$D = \lambda \frac{4(1+x_{\mathrm{bb}})}{\pi x_{\mathrm{bb}}^2}\left[x_{\mathrm{bb}} - \ln(1+x_{\mathrm{bb}}) - \frac{x_{\mathrm{bb}}^2}{2(1+x_{\mathrm{bb}})}\right] \tag{27}$$

where x_{bb} is normalized strain amplitude, $\lambda = \pi D_{\max}/2$. Eq. (27) is good approached by suitable choice of constants in Eq. (23) for the new model, e.g. for $D_{\max} = 0.3$ the constants provided good approximation

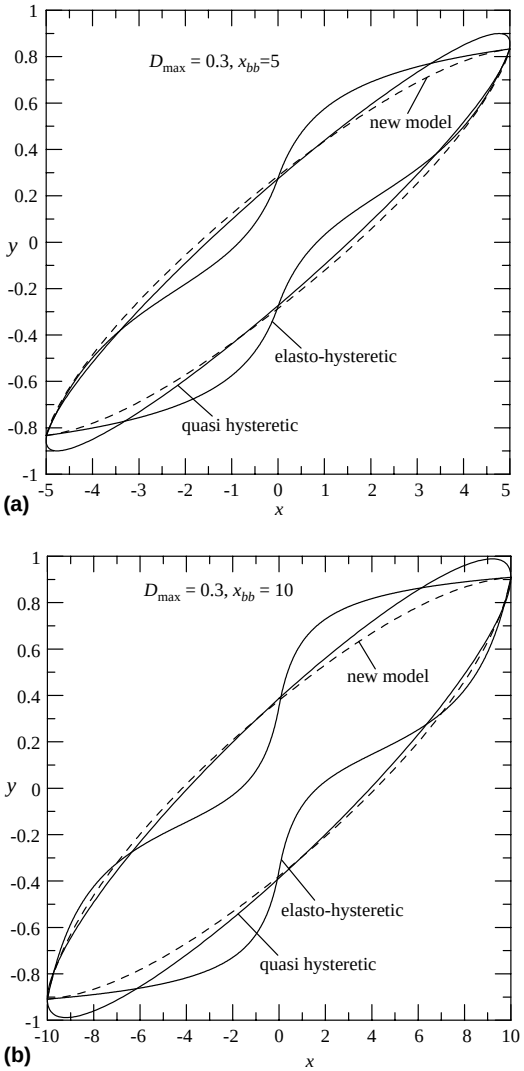

Fig. 8. Forms of hysteretic loops for three considered models for $x_{\mathrm{bb}} = 5$ (a) and 10 (b); $D_{\max} = 0.3$.

are: $A = 13.7$, $B = 18.9$. For the quasi hysteretic model the dependence (27) can be introduced into calculations directly. In Fig. 8(a) and (b) hysteretic loops are shown for values $x_{bb} = 5$, 10 and $D_{max} = 0.3$. Note that in the case of quasi hysteretic model the elliptical loop is established for sinusoidal strain variation after a number of cycles, whereas for the two remaining models one cycle is enough for obtaining the hysteretic loop. All three loops have practically equal area. Apparently, the loop shape corresponding to the model suggested in this paper is more suitable for describing experimental results for soils than shapes obtained in the other two models.

For illustration how the damping influences the response of a non-linear hysteretic mechanical system in dynamics consider some examples. Let a mass m be attached to a spring which obeys the non-linear hysteretic stress–strain relationship. We keep notations G_{max}, τ, γ for the initial stiffness, force, displacement,

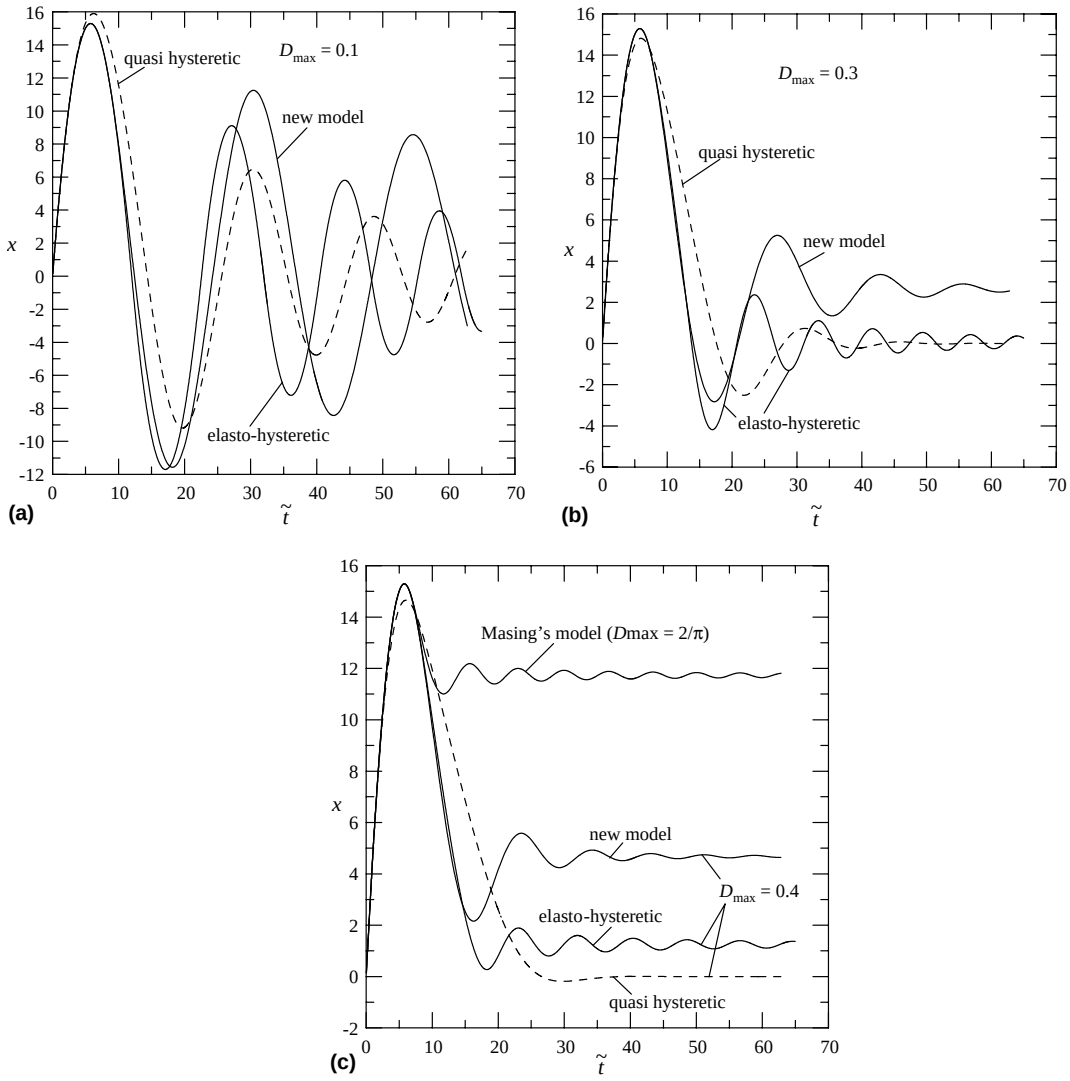

Fig. 9. Response of hysteretic models on an instantaneous impulse for three values of $D_{max} = 0.1$ (a), 0.3 (b), 0.4 (c); initial derivative is equal to 5.

respectively (as the 'spring' one can image a shear rod which has square cross section with unit sides). Equation of motion has the form

$$m\ddot{\gamma} + \tau = T \tag{28}$$

where T is an external force. Using the normalized values x and y according to (3) and the non-dimensional time

$$\tilde{t} = t\sqrt{\frac{G_{\max}}{m}} \tag{29}$$

leads to

$$\frac{\mathrm{d}^2 x}{\mathrm{d}\tilde{t}^2} + y = \widetilde{T} \tag{30}$$

where $\widetilde{T} = T/\tau_u$. This equation was solved numerically in the case of hyperbolic backbone curve (2) for the three considered models in the case of $T = 0$, $x(0) = 0$ and value of initial derivative $\mathrm{d}x/\mathrm{d}\tilde{t}$ equal to 5 (action of an instantaneous impulse); maximum values of damping ratio are $D_{\max} = 0.1, 0.3, 0.4$ with the damping dependence on normalized amplitudes according to (27). In the case of quasi hysteretic model parameter n entering the mean value definition (26) is taking equal to 2. Numeric integration is carried out using method of constant mean accelerations (a particular case of the well known Newmark's method) with iterations. The four extended rules with the constructed hysteresis function $\Phi(u)$ (instead of the scaled backbone function) allow us to compute forces (and therefore accelerations from (30)) knowing displacements at the end of an integration step for the each iteration. In turn, these displacements (and also velocities) are found from relationships of the method of constant mean accelerations using the known state at the beginning of the time step and end acceleration. The latter is set previously equal to the initial (at the step beginning) acceleration and then is defined more exactly by iterations. One can find brief description of the algorithm (for quasi hysteretic model) in papers by Muravskii (2004) and Muravskii and Frydman (1998). Results of calculations are represented in Fig. 9(a)–(c) for the indicated values of $D_{\max}$, respectively. In Fig. 9(c) also the plot corresponding to the pure Masing's model ($D_{\max} = 2/\pi$) is shown; to this plot should tend (with

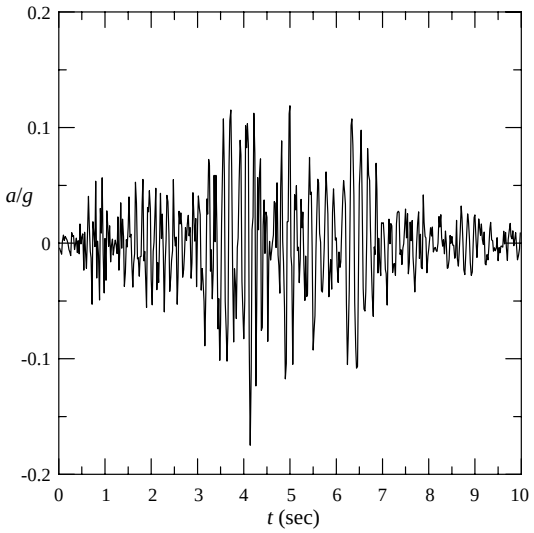

Fig. 10. Input accelerogram at rock outcrop.

increase in $D_{\max}$) plots corresponding to the new model and the elasto-hysteretic model. Because of discrepancies in the form of hysteretic loops for these two models the responses on the impulse action differ significantly after the first period of vibration. In the example, the elasto-hysteretic model leads to practically zero residual displacements even for $D_{\max} = 0.3$, and only for greater values of $D_{\max}$ the noticeable residual displacements occur. For the quasi hysteretic model displacements after impulse action tend with time to zero.

Further consider an example of seismic response analysis for a 50 m sand layer having a density $\rho = 2000\,\mathrm{kg}/m^3$. The layer is connected at its bottom to bedrock. We take the following values for the shear strength τ_u and the initial modulus $G_{\max}$ of soil at the depth $H = 50\,\mathrm{m}$: $\tau_u(H) = 170\,\mathrm{KPa}$, $G_{\max}(H) = 200$ MPa. The following behaviour of values τ_u and $G_{\max}$ with depth h is assumed

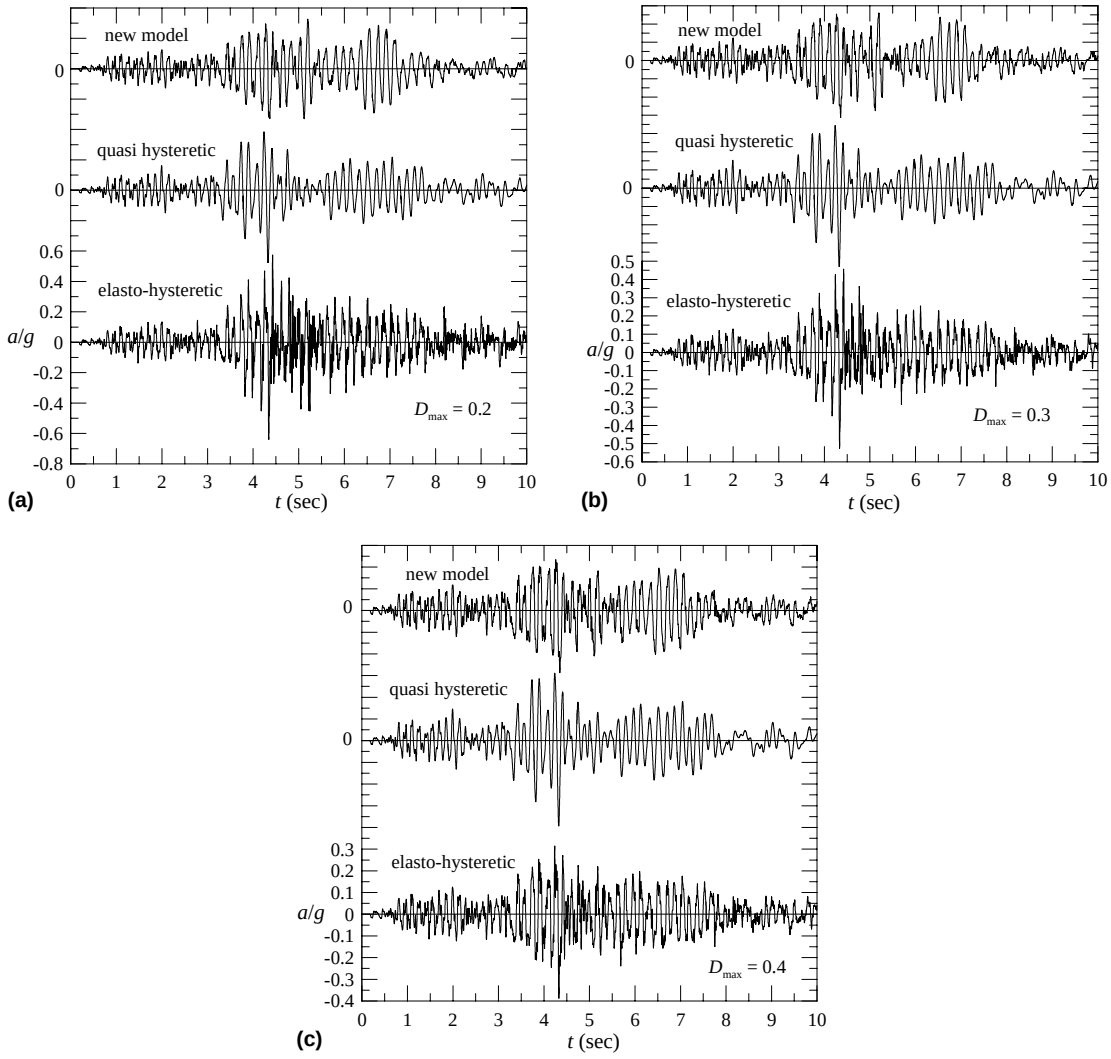

Fig. 11. Surface accelerations for three hysteretic models for values of maximum damping ratio 0.2 (a), 0.3(b) and 0.4(c); backbone curve is hyperbolic.

$$\tau_u(h) = \tau_u(H)\frac{0.2 + h/H}{1.2} \tag{31}$$

$$G_{\max}(h) = G_{\max}(H)\sqrt{\frac{0.2 + h/H}{1.2}} \tag{32}$$

The earthquake vibration input at rock outcrop is the E–W record of the October 1, 1987 Whittier earthquake, recorded at the Mt. Wilson–Caltech Seismic Station (maximum acceleration $0.175g$), the corresponding accelerogram is represented in Fig. 10. A one-dimensional problem associated with propagation of shear waves through the soil layer is studied. In calculations, the interaction between the bedrock (which is assumed as elastic with shear modulus G_R and density ρ_R) and the soil layer is considered; the ratio of the value $G_R\rho_R$ to the value $G_{\max}(H)\rho$ is taken equal to 75.

The backbone curve (normalized) is chosen in the form of hyperbola (2), the value of $D_{\max}$ is assumed to be constant in the layer; the dependence of the damping ratio on strain amplitude for the three considered models corresponds to the elasto-hysteretic model, i.e. to Eq. (27) (for the hyperbolic backbone curve). The problem is solved by dividing the soil layer into N elements and referring to displacements of nodal points u_j ($j = 0, \ldots, N$). The distribution of displacements within elements is assumed to be linear, leading to constant values of strain. Mass is concentrated at nodes, and, when writing equations of motion for nodes, stresses are taken in middle points of elements. For integration in time, the method of constant average accelerations with iterations is used (as above in the case of single-degree-of-freedom system). Calculations have shown that the value $N = 50$ along with the time step $\Delta t = 0.00025\,\mathrm{s}$ provide a good precision by solving the problem. When using the quasi hysteretic model we take $n = 2$ in Eq. (26) giving more relative weight to data close to current time t, which leads to a quicker response of material characteristics on changes in the level of deformation. In Fig. 11 accelerations at the soil surface are represented for values of maximum damping ratio $D_{\max} = 0.2$, 0.3, 0.4. The influence of the damping on peak values of output acceleration is especially high for elasto-hysteretic model: amplification factor (ratio of maximum output and input accelerations) decreases for this model from 3.65 to 2.22 with increase in $D_{\max}$ from 0.2 to 0.4. The corresponding values of the amplification factor are 2.72 and 2.24 for quasi-hysteretic model and 1.89 and 1.64 for the

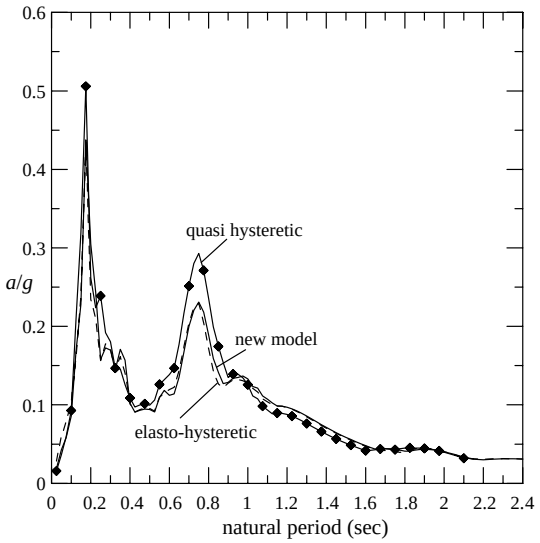

Fig. 12. Pseudo accelerations at 5% damping corresponding to surface accelerations of Fig. 11(c).

new model. The results for the three models become closer to each other with increase in the damping ratio. General pattern of the response are similar for the three models which is exhibited in proximity of pseudo accelerations (Newmark and Rosenbluet, 1971) which are represented for the three models in Fig. 12 for surface accelerations of Fig. 11(c).

4. Introducing hysteresis properties of material into system with constant stiffness

In the case with backbone curve having the form of a straight line (case of constant stiffness), formal application of original Masing's rules leads to a linear non-dissipative system and therefore is senseless. However the hysteresis function Φ which does not depend on backbone curve can be used in the considered case and also in the case of stiffness increasing with increase of deformation. Consider the backbone curve in the form

$$\tau = G_0\gamma \tag{33}$$

where G_0 is the constant stiffness. When constructing the function Φ, the four extended Masing's rules with modified second rule according to Eq. (4) are retained. The requirements (ii) and (iv) in (6) are changed as follows:

$$\begin{aligned} &\text{(ii)}\ \Phi'(0) = \mu_1 G_0 \\ &\text{(iv)}\ \Phi'(2\gamma_{bb}) = \mu_2 G_0 \end{aligned} \tag{34}$$

where coefficients μ_1 and μ_2 with the properties: $\mu_1 > 1$, $0 < \mu_2 < 1$ are introduced. Making the hysteretic loops nearly symmetrical regarding to the straight line (33) we adopt $\mu_1 = 1/\mu_2$. Taking the hysteresis function according to (13), let us set the parameter $q = 15$ and apply a parameter, α, which determines the value $\Phi(\gamma_{bb})$ (in the middle point of the interval $0 < \gamma < 2\gamma_{bb}$) as follows:

$$\Phi(\gamma_{bb}) = G_0(1+\alpha)\gamma_{bb} \tag{35}$$

Note that $0 < \alpha < 1$. The parameters influencing function $\Phi(u)$ are represented in Fig. 13 where the upper part of a hysteretic loop formed by the function is shown. Numerous calculations show that the following relationship between parameters μ_2 and α is appropriate

$$\mu_2 = 0.02\alpha + (1-\alpha)^5 \tag{36}$$

So we can construct a family of hysteretic models and corresponding hysteretic loops depending on parameter α, which influences the form of the loops and the damping ratio. Parameter R is determined using other parameters and the function value at an intermediate point (Muravskii, 1996), i.e. value $\Phi(\gamma_{bb})$ by (35), in the form which does not contain G_0 and γ_{bb}

$$R = \ln\frac{(1-\mu_2)[(\mu_1-\mu_2)(1+q-0.5^q)-(1+q)(1+\alpha-\mu_2)]}{(1+\alpha-\mu_2)[(\mu_1-\mu_2)q-(1+q)(1-\mu_2)]} \Big/ \ln\frac{1+q-0.5^q}{2q} \tag{37}$$

Considering function (13) it can be shown that for applied assumptions the hysteresis function can be represented in the form

$$\Phi(u) = G_0\gamma_{bb}\Phi_0(u/\gamma_{bb}) \tag{38}$$

where the function $\Phi_0(u)$ corresponds to the values $G_0 = 1$, $\gamma_{bb} = 1$. From this the damping ratio independence of strain amplitude γ_{bb} and stiffness G_0 follows, thus only two parameters, G_0 and D, are inherent in the considered hysteretic system. Carrying out calculations for values of parameter α from the interval $0 < \alpha < 1$ and determining corresponding values of damping ratio D, the dependence of parameter α on damping ratio is obtained. The corresponding relationship is shown in Fig. 14. Very precise approximation for this function is realized by the following equation of the type (13):

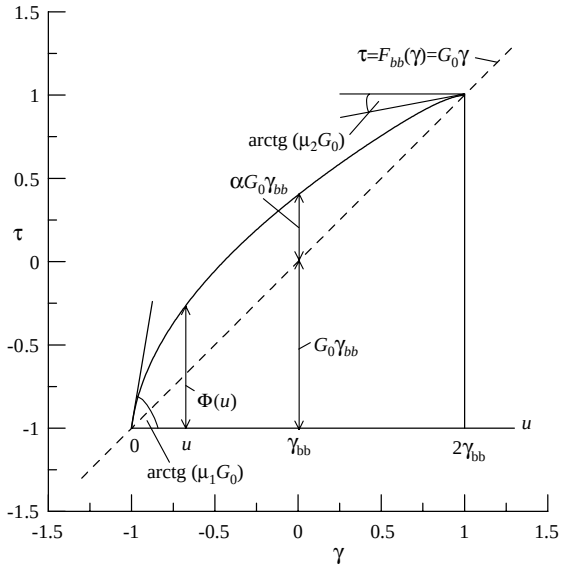

Fig. 13. On constructing function $\Phi(u)$ for model with constant stiffness.

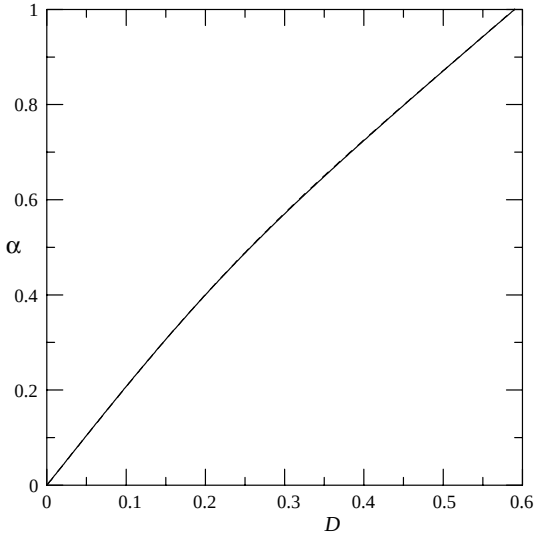

Fig. 14. Dependence of parameter α on damping ratio.

$$\alpha = 1.438D + \frac{0.6485D(1 - 0.957D^2)}{1 + 7.67(D - 0.957D^3)^{2.6}} \tag{39}$$

The curve corresponding to this equation and the original calculated curve in Fig. 14 are practically indistinguishable (discrepancies are less than 0.25%). Note that $\alpha \approx 2D$ for small values of D.

For a given value of D, the parameter α can be found by (39) and μ_2 by (36). Taking $q = 15$, $\mu_1 = 1/\mu_2$ and defining R by (37), all parameters determining the function $\Phi_0(u)$ according to (13) are available

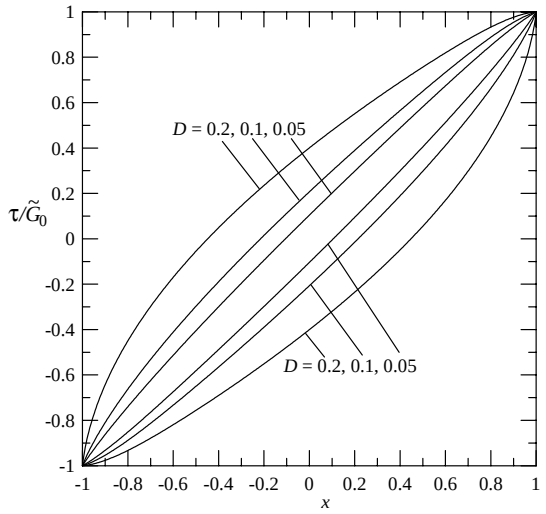

Fig. 15. Hysteretic loops for model with constant stiffness for 3 values of $D = 0.05, 0.1, 0.2$.

independently of strain history. Fig. 15 illustrates hysteretic loops obtained according to the described procedure for 3 values of $D = 0.05, 0.1, 0.2$. The normalized strain x used in this illustration can be defined as the original strain γ divided by a reference strain γ_r (e.g. $\gamma_r = 0.001$) with the corresponding change of G_0 to $\widetilde{G}_0 = G_0\gamma_r$. The recalculated (after the function $\Phi_0(u)$ has been constructed) values of D are 0.04990, 0.09979, 0.2002, respectively. This gives estimation for the error entered by application of Eq. (39). Fig. 16 illustrates all the extended Masing's rules for a relationship between strain and stress for a given strain history; again a normalized strain x is used. Determination of the parameter $\gamma_{bb}(x_{bb})$, influencing the function Φ at the next stage of the motion, takes place in the points A, E, G.

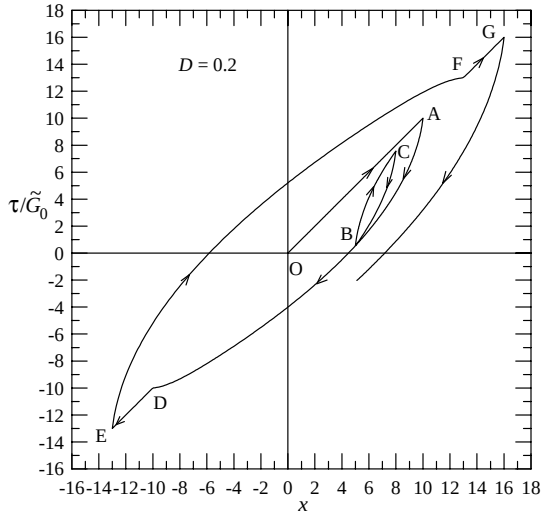

Fig. 16. Stress–strain relationship illustrating four extended Masing's rules for model with constant stiffness.

The property of the hysteresis function expressed in Eq. (38) leads to partial linearity of the considered system. It can be shown that for two strain histories, $\gamma_1(t)$ and $\gamma_2(t) = C\gamma_1(t)$, where C is a constant, the corresponding stresses will be in the same proportion: $\tau_2(t) = C\tau_1(t)$. This property allows us to consider, for example, the response of the system on the unit instantaneous impulse and use the corresponding proportion for an arbitrary impulse value. Analogously, when studying steady state vibrations under action of a harmonic force, one can consider only unit force amplitude. Thus it is possible to compare in some cases the considered non-linear system with linear one. The constructed hysteresis model can serve as a suitable model for taking account on frequency independent damping supplementing results given in paper by Muravskii (2004).

Consider one example for a one-degree-of-freedom system. Using Eq. (28) we make variable change (29) but with G_0 instead of $G_{\max}$. The equation of motion can be written in the form

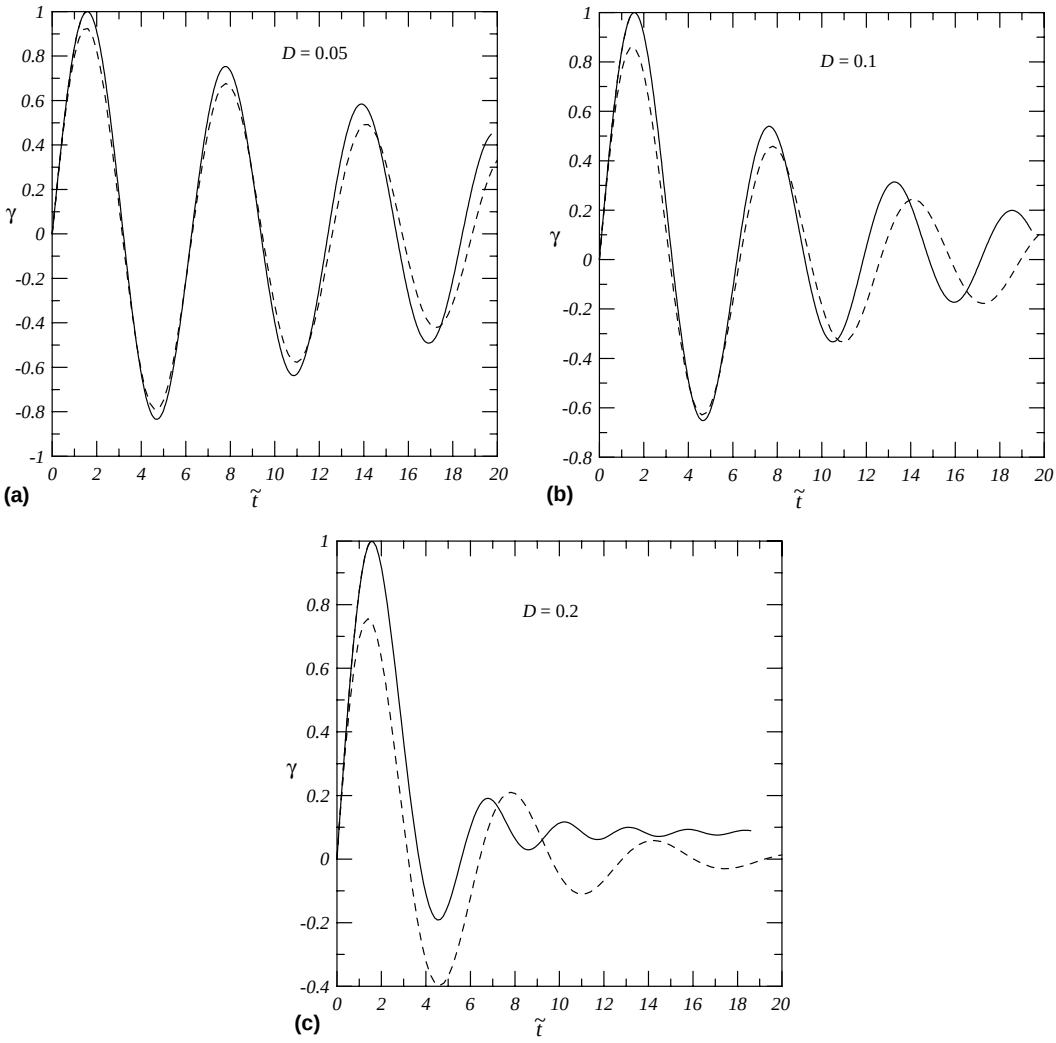

Fig. 17. Response of hysteretic models with linear backbone curve on an instantaneous impulse for three values of $D_{\max} = 0.05$ (a), 0.1 (b), 0.2 (c); initial derivative is equal to 1.

$$\frac{\mathrm{d}^2\gamma}{\mathrm{d}\tilde{t}^2} + \tilde{\tau} = \widetilde{T} \tag{40}$$

where the tilde denotes that the corresponding forces are divided by G_0 i.e. the 'spring' reaction $\tilde{\tau}$ corresponds now to unit value of stiffness. Consider the action of an instantaneous impulse with $T = 0$, $\gamma(0) = 0$ and the value of initial derivative $\mathrm{d}\gamma/\mathrm{d}\tilde{t}$ equal to 1. The displacements for values of damping ratio $D = 0.05$, 0.1, 0.2 are shown in Fig. 17. For comparison, the results corresponding to a linear model with viscose damping are represented in the figure (dashed lines). For this model

$$\tau = G_0\gamma + \mu\frac{\mathrm{d}\gamma}{\mathrm{d}t} = G_0\left(\gamma + 2\xi\frac{\mathrm{d}\gamma}{\mathrm{d}\tilde{t}}\right) \tag{41}$$

where coefficient μ is a constant and

$$\xi = \frac{\mu}{2\sqrt{mG_0}} \tag{42}$$

In calculations damping parameter ξ is taken equal to D which leads to the linear model 'equivalent' to original non-linear hysteretic model. The results of calculations are rather close for the two models in the case of small damping. With increase of damping the discrepancies become noticeable: for the hysteretic model the first maximum of displacements does not depend on damping whereas the residual displacement increases with increase in damping ratio. The linear viscose system has no residual displacement, and the damping leads to decrease in the first maximum of displacements.

5. Concluding remarks

The hysteretic models developed in the paper are based on the well known four extended Masing's rules with using a general function for constructing loading and reloading curves, as an alternative to the scaled backbone curve inherent in Masing's rules. This allows us to match more flexible the theoretical results to experimental data, particularly to regulate damping properties of the model. In the case of backbone curve with limited stress, the requirements imposed on the hysteresis function are identical to the conditions satisfied by scaled backbone curve besides the behaviour in intermediate points of hysteretic loops. The model is able to provide the required maximum value of the damping ratio as well as the behaviour of the damping ratio at small and intermediate values of the strain amplitude. In the case of the backbone curve in the form of a straight line, the hysteretic model possesses the property of partial linearity which makes it possible to compare in some cases the hysteretic model with corresponding linear models. Damping ratio is in this case an independent model parameter which is not influenced by the strain amplitude.

References

Archuleta, R.J., Bonilla, L.F., Lavallée, D., 1999. Nonlinear site response using generalized Masing rules coupled with pore pressure. In: Proceedings of the OECD-NRC Workshop on Engineering Characterization of Seismic Input. Brookhaven National Laboratory, New York.

Bouc, R., 1967. Forced vibration of mechanical system with hysteresis. In: Proceedings of the 4th Conference on Non-linear Oscillation, Prague. pp. 315–315.

Davidenkov, N.N., 1938. Energy dissipation in vibrations. Journal of Technical Physics 8 (6) (in Russian).

Goodier, J.N., Hodge Jr., P.G., 1958. Elasticity and Plasticity. John Wiley and Sons Inc., NY.

Hardin, B.O., Drnevich, V.P., 1972a. Shear modulus and damping in soils: measurement and parameter effects. Journal of the Soil Mechanics and Foundations Division, ASCE 98 (6), 603–624.

Hardin, B.O., Drnevich, V.P., 1972b. Shear modulus and damping in soils: design equation and curves. Journal of the Soil Mechanics and Foundations Division, ASCE 98 (7), 667–692.

Iwan, W.D., 1966. A distributed element model for hysteresis and its steady-state dynamic response. Journal of Applied Mechanics 33, 893–900.

Iwan, W.D., 1967. On a class of models for the yielding behaviour of continuous and composite systems. Journal of Applied Mechanics 34, 612–617.

Kramer, S.L., 1996. Geotechnical Earthquake Engineering. Prentice-Hall, Upper Saddle River, NJ.

Masing, G., 1926. Eigenspannungen und Verfestigung beim Messing. In: Proceedings of the 2nd International Congress on Applied Mechanics, Zürich. pp. 332–335.

Muravskii, G., 1994. Frequency independent model for damping. In: Proceedings of the 25th Israel Conference of Mechanical Engineering, Haifa, Israel. pp. 230–232.

Muravskii, G.B., 1996. On analytical description of stress–strain relationship for rocks and soils. Communications in Numerical Methods in Engineering 12, 827–834.

Muravskii, G.B., 2001. Application of experimental results on cyclic deforming of soils to seismic response analysis. Soil Dynamics and Earthquake Engineering 21, 661–669.

Muravskii, G.B., 2004. On frequency independent damping. Journal of Sound and Vibration 274, 653–668.

Muravskii, G., Frydman, S., 1998. Site response analysis using a nonlinear hysteretic model. Soil Dynamics and Earthquake Engineering 17, 227–238.

Newmark, N.M., Rosenblueth, E., 1971. Fundamentals of Earthquake Engineering. Prentice-Hall, Englewood Cliffs, NJ.

Osinov, V.A., 2003. Cyclic shearing and liquefaction of soil under irregular loading: an incremental model for the dynamic earthquake-induced deformation. Soil Dynamics and Earthquake Engineering 23, 535–548.

Puzrin, A.M., Burland, J.B., 1996. A logarithmic stress–strain function for rocks and soils. Geotechnique 46 (1), 157–164.

Pyke, R., 1979. Nonlinear soil model for irregular cyclic loadings. Journal of the Geotechnical Engineering Division, ASCE 105, 715–726.

Shames, I.H., Cozzarelli, F.A., 1992. Elastic and Inelastic Stress Analysis. Prentice Hall, Englewood Cliffs, NJ.

Visintin, A., 1994. Differencial Models of Hysteresis. Springer-Verlag, Heidelberg, Germany.

Wen, Y.K., 1976. Method for random vibration of hysteretic systems. Journal of the Engineering Mechanics Division, ASCE 102 (2), 249–263.